Biophysical Journal Volume 109 October 2015 1338–1346

Article

A Kinetic Model for Cell Damage Caused by Oligomer Formation

Liu Hong,[1,*] Ya-Jing Huang,[1] and Wen-An Yong[1]

[1]Zhou Pei-Yuan Center for Applied Mathematics, Tsinghua University, Peking, P.R. China

ABSTRACT It is well known that the formation of amyloid fiber may cause invertible damage to cells, although the underlying mechanism has not been fully understood. In this article, a microscopic model considering the detailed processes of amyloid formation and cell damage is constructed based on four simple assumptions, one of which is that cell damage is raised by oligomers rather than mature fibrils. By taking the maximum entropy principle, this microscopic model in the form of infinite mass-action equations together with two reaction-convection partial differential equations (PDEs) has been greatly coarse-grained into a macroscopic system consisting of only five ordinary differential equations (ODEs). With this simple model, the effects of primary nucleation, elongation, fragmentation, and protein and seeds concentration on amyloid formation and cell damage have been extensively explored and compared with experiments. We hope that our results will provide new insights into the quantitative linkage between amyloid formation and cell damage.

INTRODUCTION

Since the first discovery of prions by Prusiner in 1982 (1), more than 20 different kinds of human neuron-degenerative diseases, such as the most well-known Alzheimer's and Parkinson's diseases, have been identified to be correlated with the abnormal accumulation of amyloid proteins and fibrils in tissues (2). As a result, to quantify the relationship between the processes of amyloid formation and cell damage has become a central task in this field.

As a typical self-assembling biosystem, the study of amyloid fiber has a long history and has attracted broad interests. Pioneer works date back to Oosawa for his studies on actins in the late 1950s (3). Later, the roles of conformational transition, primary nucleation, and elongation during the formation of amyloid formation were gradually explored and characterized (4). Hofrichter, Eaton, and Ferrone found that surface-catalyzed secondary nucleation is crucial for several amyloid proteins, e.g., sickle-cell hemoglobin and $IAPP_{20\text{-}29}$ (5-7). Although fragmentation as an alternative way for secondary nucleation was already mentioned in Oosawa's famous book (8), corresponding detailed experimental (9,10) and mathematical analyses (11,12) have not been carried out until the beginning of new era. Now we are at a stage to interpret and predict various kinetic and thermodynamic data in real-time with high precision (13,14), which provides a solid starting point for our current study.

For quite a long time, mature fibrils have been taken for granted as the major cause of cell damage, and the fiber concentration in tissues was regarded as a key factor to quantify the progress of amyloidosis (12,15). In general, the more fibrils deposit, the greater toxicity will affect the cells. However with accumulative evidences on the morphology, structure, and function of oligomers and fibrils both in vitro and in vivo (16,17), this view has been largely changed in recent years. Now heterogeneous oligomers are generally considered far more toxic to cells than mature fibrils. A prominent hypothesis suggests that in cells the exposed flexible hydrophobic surfaces of oligomers can mediate aberrant interactions with other proteins, resulting in their functional impairment (2,18). As a result, the toxicity of oligomers is highly correlated with their capacity to promote aberrant protein interactions and to deregulate the cytosolic stress response (19). Another possible mechanism may be due to the interaction between oligomers and the cell membrane. Once oligomers bind onto the membrane, they may dramatically change the local geometry, electricity, and permeability of the membrane, which will lead to the local destabilization, permeation, and even rupture of the latter (20,21). In addition, oligomers may also form unintended pores or ion-channel-like structures in the membrane and thus give rise to fatal abnormal ion leakage of the cell (22,23). For instance, Demuro observed in *Xenopus* oocytes that Aβ (1-42) oligomers can lead to abnormal Ca^{2+} flux independent of ion-channel from 5 to 40 mer (24). Schauerte further pointed out that hexamer is the smallest stable oligomer that can penetrate the cell membrane, whereas 12 to 14 mer give rise to the largest ion current (25).

In this study, we attempt to characterize the cell damage caused by oligomers quantitatively, especially to link the cytotoxicity with the progress of amyloid formation based on several simple assumptions. Despite extensive studies

Submitted December 17, 2014, and accepted for publication August 11, 2015.

*Correspondence: zcamhl@tsinghua.edu.cn

Editor: Gijsje Koenderink

0006-3495/15/10/1338/9

http://dx.doi.org/10.1016/j.bpj.2015.08.007

on the formation of amyloid fiber, relatively limited research has been performed on this aspect (26,27). Considering the microscopic processes of amyloid formation and cell damage, our model is formulated through a group of coupled mass-action equations and reaction-convection equations. By using the method of maximum entropy principle, our derived model is greatly simplified into five macroscopic moment-closure equations, which are ordinary differential equations (ODEs) and easy to solve. Detailed model analyses and comparisons with experimental data are also highlighted.

This article is organized as follows. First, we introduce our four basic assumptions. Then we describe a general framework of our mathematical model and our simplified moment-closure equations. Further numerical validations are shown in Fig. 2. The original mass-action equations plus two reaction-convection equations and the method we used for deriving the moment-closure equations (maximum entropy principle) are left to the Supporting Material. Interested readers can find all necessary details there. In the following, our main results are separated into several parts. With the moment-closure model, the effects of primary nucleation, elongation, fragmentation, and protein and seeds concentration on amyloid formation and cell damage are extensively explored and compared with the experiments. In addition, several interesting scaling laws for important kinetic quantities are mentioned. We address further discussions in the end.

MATERIALS AND METHODS

The processes of amyloid formation and cell damage are closely correlated, during which oligomers play a key role

It is widely known that the processes of amyloid formation and cell damage are closely correlated, but the underlying quantitative relations have never been clarified. To solve this problem, we construct a microscopic mathematical model, which relies on the following four basic assumptions:

1) The basic procedure of amyloid formation can be well characterized through a kinetic model, which includes primary nucleation, elongation, and fragmentation, as well as their corresponding inverse processes. Oligomers act as on-pathway intermediates or building blocks of fibrils;
2) Cell toxicity is mainly caused by oligomers, rather than mature fibrils and monomers, through their binding to the cell membrane. The more oligomers have bound, the greater damage to the cell membrane would occur;
3) Ion concentration inside a cell can be used as an effective index to quantify the cytotoxicity. Besides normal ion exchanges, the appearance of abnormal ion leakage depends on the degrees of how the cell membrane is damaged; and
4) Oligomer binding does not apparently influence the kinetics of amyloid formation. In other words, in this study we neglect the consumption of oligomers during their interactions with the cell membrane.

The first assumption points out the possible mechanisms for amyloid formation. Based on our studies and other related works (11,12), most observations on amyloid formation can be well interpreted by this kind of model. The necessities of surface-catalyzed secondary nucleation (28), thickening (29,30), protein diffusion (31), and so on are left to future studies. In this study, for simplicity, oligomers are modeled as on-pathway intermediates; however, in many amyloid-related diseases cytotoxic oligomers are shown to be off-pathway aggregates, which means conformational transition (32,33) or off-pathway polymerization (34) should be considered as important generalizations in the next step. The next two assumptions point out possible candidates for cytotoxicity. Although at a first glance, amyloidosis can be linked easily with the deposit of fibrils, accumulative evidences in recent years have gradually changed this view and revealed that oligomers may be the prime pathogenic factor instead. The cytotoxicity of monomers and fibrils are often negligible compared with that of oligomers (35,36). In this study, we make a further assumption on the detailed mechanism of cytotoxicity, including oligomer binding, cell membrane damage, and ion leakage. The final cytotoxicity is quantified through the leaked ion concentration from the inside cell. The last one assumes that the processes of amyloid formation are independent of oligomer binding. In other words, we neglect the consumption of oligomers during their interactions with the cells. Although it seems to be a very rough approximation, it works in many cases once binding does not cause apparent loss of oligomers. As we will show, this assumption helps us greatly to simplify the mathematical modeling and computation.

The kinetics of amyloid formation and cell damage both can be well modeled through a series of chemical reactions

Based on our assumptions above, two basic procedures should be considered to model the kinetics of cell damage caused by amyloid formation: one is the formation of oligomers and fibrils; the other is the change of ion concentrations inside a cell, which is caused by the damage of cell membrane through oligomer binding (see Fig. 1).

The modeling of the first procedure has been well established in the past studies (8,11,12). Primary nucleation, elongation, and fragmentation are generally considered as the three basic processes in this part. To be exact, we assume that monomers first aggregate into oligomers through primary nucleation with the critical size as n_c. Then on-pathway oligomers grow into mature fibrils by elongation. Once oligomers and fibrils exceed a certain given size, they may break into two small pieces spontaneously. To sum up, this part is modeled through following chemical reactions:

$$\begin{aligned} n_c A_1 &\underset{k_n^-}{\overset{k_n^+}{\rightleftharpoons}} A_{n_c}, \\ A_1 + A_i &\underset{k_e^-}{\overset{k_e^+}{\rightleftharpoons}} A_{i+1}, \\ A_{i+j} &\underset{k_f^-(i,j)}{\overset{k_f^+(i,j)}{\rightleftharpoons}} A_i + A_j, \quad (i,j \geq n_c) \end{aligned} \tag{1}$$

where k_n^+ and k_e^+ are the forward reaction rate constants for fiber primary nucleation and elongation respectively; k_n^- and k_e^- are the corresponding backward ones; $k_f^+(i,j)$ and $k_f^-(i,j)$ are length-dependent reaction rate constants for fiber fragmentation and association, whose formulas are taken according to the Hill's model (37); A_1 stands for monomers; and A_i stands for oligomers or fibrils of size i. Here oligomers are modeled as on-pathway building blocks of fibrils rather than off-pathway aggregates. They are supposed to be small aggregates with sizes varying from n_c to n_o and can cause cytotoxicity; whereas

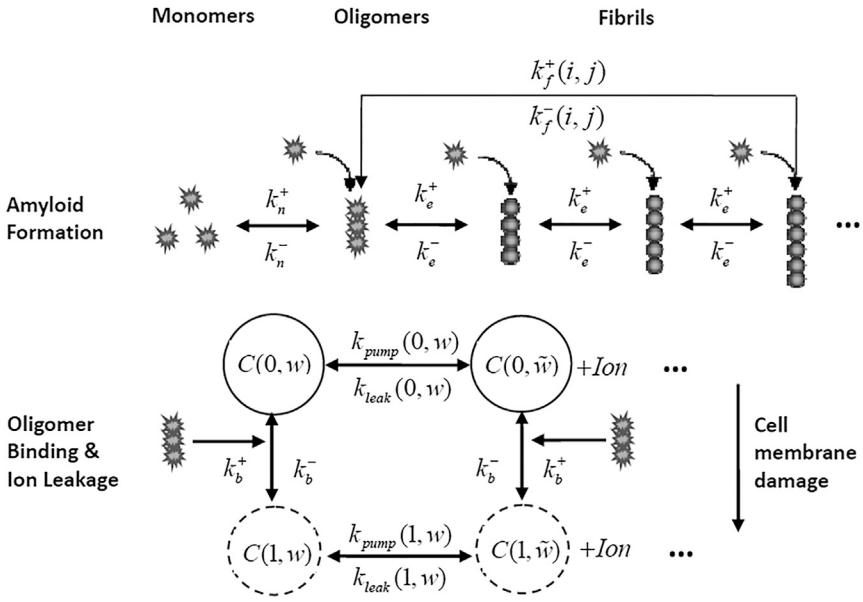

FIGURE 1 An illustration of our kinetic model with oligomer size as 3.

fibrils have sizes larger than n_o and are not harmful to cells. Therefore, we make a distinction between oligomers and fibrils based on their respective sizes and functions rather than the morphology and reaction rates. The above descriptions actually provide a practical rather than precise definition of oligomers and fibrils.

In the second part of our model, we need to link the oligomer concentration with the cytotoxicity quantitatively. Indeed, the concentration of bound oligomers on the membrane is a key determinant of the future of the cells. But because of the lack of direct observations until now, if we want to quantify the cytotoxicity, additional assumptions on what happens after oligomer binding (or relations between the concentration of bound oligomers and cytotoxicity) are still needed.

As many recent studies have revealed (27,38), the binding of oligomers onto the cell membrane may cause the local destabilization and permeation of the latter or form unintended pores, giving rise to abnormal leakage of ions (especially Ca^{2+}) and eventually the death of cells. According to this general picture, we denote the cells by $C(s,w)$, where $s=0/1$ and $w\in[0,1]$. The first index characterizes the damaged condition of a cell. Here for simplicity, a two-valued variable is considered, i.e., $s=0$ stands for the normal cellular state, and $s=1$ stands for the totally damaged state. However, it is not difficult to generalize this approach into a continuous version by taking in other intermediate cellular states (see the Supporting Material). Different cellular states can converge into each other through oligomer binding and unbinding, whose reaction rate constants are given through k_b^+ and k_b^- respectively, as follows:

$$C(0,w) \underset{k_b^-}{\overset{k_b^+(+A_i)}{\rightleftharpoons}} C(1,w). \quad i\in[n_c,n_o]. \qquad (2)$$

We note that the forward process depends on the oligomer concentration, whereas the backward one does not (because of the very weak and slow self-healing of the membrane).

The second index w shows the normalized ion concentration inside a cell, which can be taken as an effective quantity to measure the cell damage caused by amyloid formation and is directly related to most popular experiments on cytotoxicity. The changes of ion concentrations inside a cell can be attributed to inward and outward ion fluxes, both of which depend not only on the ion concentration gradient between cell and environment, but also on the cellular state as follows:

$$C(s,w) \underset{k_{pump}(s,w)}{\overset{k_{leak}(s,w)}{\rightleftharpoons}} C(s,w')+(w-w')Ion, \qquad (3)$$

where $k_{leak}(s,w)$ is the ion leakage rate because of cell membrane damage, and $k_{pump}(s,w)$ is the speed of ion pumps that try to maintain a constant internal ion concentration w. Here for simplicity, only linear constitutive relations are considered, i.e., $k_{pump}(s,w)=2k_{pump}\times(1-w)\delta_{s,0}$ and $k_{leak}(s,w)=2k_{leak}\times w\delta_{s,1}$.

Moment-closure equations provide an efficient way to quantify amyloid formation and cell damage in replace of mass-action equations

With the chemical reactions listed in Eq. 1 in hand, it is easy to formulate them into a system of ODEs according to the laws of mass action, whereas Eqs. 2 and 3 together represent two additional PDEs for oligomer binding and ion leakage. These equations together constitute the microscopic model of our current study (Eq. S1 in the Supporting Material). However, instead of bothering with these complicated formulas, we turn to much simpler moment-closure equations. Interested readers may refer to the Supporting Material for details on how to formulate mass-action equations and reaction-convection equations in a microscopic way, how to derive macroscopic moment-closure equations based on the method of maximum entropy principle, and so on.

Following the moment-closure method introduced in our previous studies (11,14), two macroscopic moments, namely the number concentration of aggregates (including both oligomers and fibrils) $P=\sum_{i=n_c}^{\infty}[A_i]$ and the mass concentration of aggregates $M=\sum_{i=n_c}^{\infty}i\cdot[A_i]$ are adopted to characterize the kinetics of amyloid formation, where $[A_i]$ stands for the concentration of aggregates of size i. Besides them, four additional quantities are introduced for cell damage and ion leakage in the same way, i.e., $C_+=\int_0^1[C(0,w,t)+C(1,w,t)]dw$, $C_-=\int_0^1[C(0,w,t)-C(1,w,t)]dw$, $I_+=\int_0^1 w[C(0,w,t)+C(1,w,t)]dw$, and $I_-=\int_0^1 w[C(0,w,t)-C(1,w,t)]dw$, where $C(0,w,t)$ and $C(1,w,t)$ stand for concentrations of normal and damaged cells with ion concentration w at time t, respectively. It is easy to note that $C_+(t)=c_{tot}$ is a constant representing the conservation of total cells.

Except for C_+ which is a constant, a self-closed system of ODEs for the other five quantities can be derived from microscopic coupled

mass-action equations and reaction-convection equations (Eq. S1) by applying the moment-closure method given in the Supporting Material as follows:

$$\begin{cases} \dfrac{d}{dt}P = k_n^+(m_{tot}-M)^{n_c} - k_n^-(1-\theta)P \\ \qquad + \displaystyle\sum_{i=n_c}^{\infty}\sum_{j=i+n_c}^{\infty} k_f^+(i,j-i)(1-\theta)\theta^{j-n_c}P \\ \qquad - \displaystyle\sum_{i=n_c}^{\infty}\sum_{j=n_c}^{\infty} k_f^-(i,j)(1-\theta)^2\theta^{i+j-2n_c}P^2, \\ \dfrac{d}{dt}M = n_c k_n^+(m_{tot}-M)^{n_c} - n_c k_n^-(1-\theta)P \\ \qquad +2k_e^+(m_{tot}-M)P - 2k_e^-\theta P, \\ \dfrac{d}{dt}C_- = -k_b^+P_{oli}(c_{tot}+C_-) + k_b^-(c_{tot}-C_-), \\ \dfrac{d}{dt}I_+ = k_{pump}(c_{tot}+C_-) - k_{pump}(I_++I_-) - k_{leak}(I_+-I_-), \\ \dfrac{d}{dt}I_- = k_{pump}(c_{tot}+C_-) - \left(k_{pump}+k_b^+P_{oli}\right)(I_++I_-) \\ \qquad +\left(k_{leak}+k_b^-\right)(I_+-I_-), \end{cases} \tag{4}$$

where $\theta \equiv (M-n_cP)/[M-(n_c-1)P] \in (0,1)$. $P_{oli} \equiv \sum_{j=n_c}^{n_o}[A_j] = \sum_{j=n_c}^{n_o}(1-\theta)\theta^{j-n_c}P$ and $M_{oli} \equiv \sum_{j=n_c}^{n_o} j\times[A_j] = \sum_{j=n_c}^{n_o} j\times(1-\theta)\theta^{j-n_c}P$ denote the number and mass concentrations of oligomers respectively. The initial conditions can be generally taken as $P(0)=M(0)=0$ and $C_-(0)=I_+(0)=I_-(0)=c_{tot}$ in the absence of initial seeds and damaged cells. The benefits of our fourth assumption can be clearly seen from above formulas, which in fact allows us to decouple the processes of amyloid formation from oligomer binding mathematically. In other words, amyloid formation manipulates the degrees of cell damage by controlling the concentration of oligomers, whereas oligomer binding has no feedback effect. This feature provides an additional advantage, too. For example, we may easily include certain levels of toxicity for monomers and fibrils, which would be a more realistic situation for Parkinson's and Alzheimer's, by simply replacing P_{oli} in Eq. 4 with other quantities.

Compared with the microscopic model (Eq. S1), our new moment-closure equations, to our knowledge, are tremendously simple. Especially the model dimension has been reduced from infinite (actually infinite-dimensional ODEs plus two PDEs) to just five (two for amyloid formation plus three for cell damage and ion leakage). As a consequence, the model computational efficiency has been improved by at least 10,000 times (from several days to seconds), which makes Eq. 4 very suitable for the real-time analysis of various experimental data on amyloid formation and correlated cell damage.

RESULTS

The kinetic essentials of amyloid formation and cell damage are well preserved by the moment-closure equations

A major difference between our model and previous ones is that there is no apparent correlation between the processes of fiber generation and cell damage. In previous studies, as mature fibrils are assumed to be responsible for cytotoxicity, the processes of fiber generation and cell damage are positively correlated. The more fibrils are formed, the more serious damage is expected be caused to cells. Contrarily in our model, according to our second assumption that monomers and mature fibrils are unharmful to cells, degrees of cell damage do not depend on the fiber concentration. Furthermore, as the oligomer concentration stays very low during the whole process of amyloid formation (compared to that of monomers and fibrils), the progress of cell damage will exhibit a sensitive dependence on the kinetic details of amyloid formation.

Are the kinetic essentials of amyloid formation and cell damage well preserved during our simplification procedure? Can the moment-closure equations honestly reflect the time-evolutionary behaviors of moments that we care about? These questions are crucial for the validity and applicability of our moment-closure equations. In Fig. 2, we carefully compare the numerical solutions of our moment-closure equations (Eq. 4) with the original coupled mass-action equations and reaction-convection equations (Eq. S1). Fig. 2, *A* and *B* clearly shows that except for the static solution of $P(t)$, whose difference is mainly caused by the exponential fiber length distribution inappropriately assumed in the moment-closure method (or in other words, the entropy function we used is not so precise), both models predict very close results. Even for the mass and number concentrations of oligomers, which play a key role in linking the two

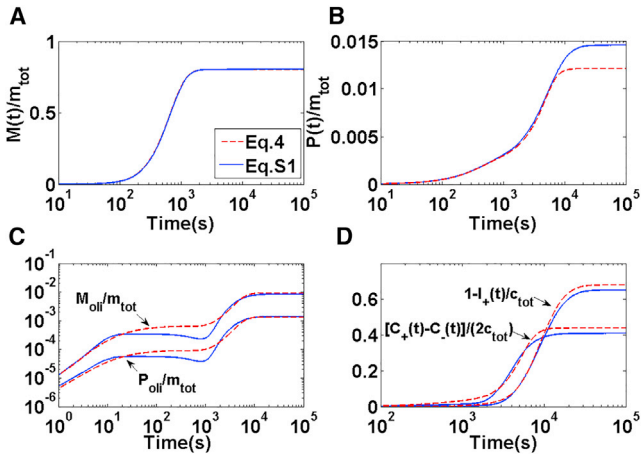

FIGURE 2 Comparisons of the moment-closure equations (Eq. 4) and microscopic model (Eq. S1) on amyloid formation and cell damage: (*A*) the mass concentration of aggregates; (*B*) the number concentration of aggregates; (*C*) the number and mass concentration of oligomers; and (*D*) the percentage of damaged cells $[C_+(t)-C_-(t)]/(2c_{tot})$ and the amount of ion leakage $1-I_+(t)/c_{tot}$. Blue solid lines stand for solutions of Eq. S1; whereas red dashed lines for solutions of Eq. 4. Here we set $m_{tot}=5\times10^{-5}M$, $c_{tot}=4.3\times10^{-5}M$, $k_n^+=0.1M^{-1}s^{-1}$, $k_n^-=0.001s^{-1}$, $k_e^+=10^4M^{-1}s^{-1}$, $k_e^-=0.1s^{-1}$, $k_f^+=10^{-4}s^{-1}$, $k_f^-=8\times10^4M^{-1}s^{-1}$, $k_b^+=10^4M^{-1}s^{-1}$, $k_b^-=10^{-3}M^{-1}s^{-1}$, $k_{pump}=5\times10^{-5}M^{-1}s^{-1}$, $k_{leak}=1.5\times10^{-4}M^{-1}s^{-1}$, $n_c=2$, $n_o=10$, and $n=1$. To see this figure in color, go online.

processes of amyloid formation and cell damage, perfect agreements are observed in the early and late time regions (Fig. 2 *C*). The only difference lies in the middle region—the exponential growth phase, during which the elongation process quickly promotes most nuclei into fibrils and thus leads to a dramatic decrease of oligomers. Despite this little disagreement in kinetics, the predictions of the moment-closure equations seem quite satisfactory on the concentration of damage cells and the amount of ion leakage through the membrane (Fig. 2 *D*). These agreements confirm the fact that the kinetic essentials of amyloid formation and cell damage in our model are well preserved during our simplification procedure. Thus the moment-closure equations provide an honest yet much efficient way to study the time-evolutionary behaviors of the important kinetic quantities that we care about.

Primary nucleation speeds up cell damage, whereas elongation generally suppresses it

Next we use our moment-closure equations to systematically investigate the effects of primary nucleation and elongation on the processes of amyloid formation and especially cell damage (see Figs. S2 and S3). With the increase of the primary nucleation rate, the speeds for fibril formation, oligomer formation, and ion leakage (or membrane leakage) grow at the same pace (35). This phenomenon is due to the fact that oligomers are modeled as on-pathway aggregates in the current case and primary nucleation is a direct way to produce them. The effect of elongation seems to be much more complicated. Roughly speaking, the elongation rate is positively correlated with the speed of fibril formation, but inversely proportional to that of oligomer formation and cell damage. Such a behavior is mainly attributable to our second assumption. If cytotoxicity is mainly caused by fibrils, then the degree of cell damage certainly will be positively proportional to the elongation rate. However, in our model cell damage is assumed to be caused by oligomers rather than fibrils. As a consequence, high elongation rate would suppress the generation of oligomers and thus the degree of cell damage in the end. With a further increase in the elongation rate, this suppression will become less and less apparent because of the limited number of oligomers (39).

Fragmentation can dramatically accelerate the formation of amyloid fiber and give rise to more serious damage to cells

As an important way for secondary nucleation, fragmentation plays a key role in the formation of breakable filaments. Once a fibril is breakable, nuclei (including ogligomers and short fibrils) can be much easier generated from long mature fibrils rather than the slow way through primary nucleation. Through such a mechanism, fragmentation can dramatically speed up the formation of fibrils and on-pathway oligomers, as well as the procedure of cell damage (see Fig. S4) (10,40). However, in the absence of initial nuclei, the influence of fragmentation is usually not as timely as the primary nucleation, because fragmentation can only be dominant once the fiber concentration exceeds certain threshold through primary nucleation.

In the past ten years, the effects of fragmentation on amyloid formation and cell damage have been widely explored in experiments. In our study, as a typical example, we apply our model to analyze the agitation data of $\beta_2 m$ fibrils performed by Xue et al. (10). Under agitation, centrifugal forces are exerted on fibrils, which will cause long fibrils to break into short pieces. From the modeling aspect, the fiber fragmentation rate grows with the increase of agitation speed. Because in this case agitation is dominated, we simply neglect the processes of primary nucleation and elongation. Fig. 3 *A* clearly shows that the average fiber length decreases monotonically during agitation, which is a strong evident for fiber breakage. Much detailed knowledge could be obtained through the fiber length distribution as shown in Fig. 3 *B*, in which the initial Gaussian-like distribution turns into an exponential distribution and more and more samples accumulate in the region of short fibrils or oligomers with the time evolving. Most importantly, under agitation the thus prepared fibrillar samples easily give rise to a high efficiency in the liposome dye release (Fig. 3 *C*). This result is consistent with the general belief that oligomers and short fibrils are much more harmful to cells than monomers and mature long fibrils (26,27).

Protein and seeds concentration have crucial influences on the kinetics of amyloid formation and cell damage

It is well known that the processes of amyloid formation and cell damage sensitively depend on the protein and seeds concentration (41). In the current case, we further address this point by examining the experiments performed by Engel et al. (42) on the kinetics of hIAPP fibril growth and hIAPP-induced membrane leakage. In Fig. 4, *A* and *B*, four different cases with initial protein concentration varying from 5 to 0.1 μM are studied by the moment-closure equations. Generally speaking, high initial protein concentration not only means short lag-time and fast fiber growth rate, but it also will lead to higher final concentrations of oligomers and fibrils and large ion leakage in the static state. Although no kinetic trace for the fibril formation is available under three low protein concentrations (except for the half-time given in Fig. 4 *C*), excellent agreements on the kinetics of fibril fromation and normalized membrane leakage still strongly confirm the reliability of our model. A further validation

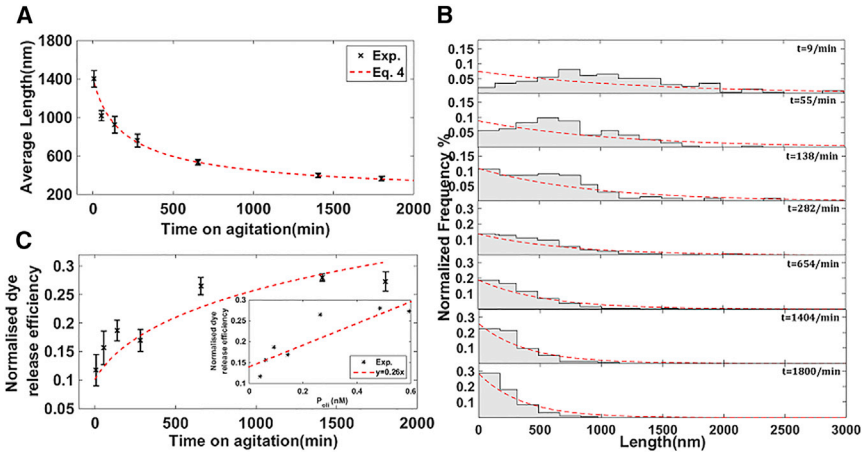

FIGURE 3 Effects of fragmentation on $\beta_2 m$ fibrils and membrane leakage: (*A*) the average fiber length under agitation; (*B*) the fiber length distribution characterized by TM-AFM; and (*C*) the amount of liposome dye release for fibrillar samples under different agitation time. Black stars with error bars stand for the data measured by Xue et al. (10); whereas red dashed lines stand for solutions of Eq. 4. Here we choose $m_{tot} = 1.2 \times 10^{-5} M$, $c_{tot} = 4.3 \times 10^{-5} M$, $k_f^+ = 2.6 \times 10^{-11} s^{-1}$, $k_b^+ = 4 \times 10^5 M^{-1} s^{-1}$, $k_b^- = 40 M^{-1} s^{-1}$, $k_{pump} = 10^{-4} M^{-1} s^{-1}$, $k_{leak} = 0.33 M^{-1} s^{-1}$, $n_c = 2$, $n_o = 40$, and $n = 3$. k_n^+, k_n^-, k_e^+, k_e^-, and k_f^- are all set to be zero. The length of one $\beta_2 m$ molecule (100 aa) along the fibril long axis is estimated as 0.41 nm. To see this figure in color, go online.

on a complete data set of the half-time between experimental data and our model predictions is available in Fig. 4 *C*. Besides the initial protein concentration, the effect of seeding on ion leakage is explored through Fig. 4 *D*, in which 0%, 1%, 2%, and 10% hIAPP seeds have been added independently to the system. It is clearly seen that high concentration of seeds dramatically speeds up the ion leakage but has little influence on the final static values as expected.

Kinetic essentials of amyloid formation and cell damage can be quantitatively learned from simple scaling relations

After a qualitative description of the kinetic behaviors of amyloid formation and cell damage, including the influences of primary nucleation, elongation, fragmentation, and protein and seeds concentration, in this section we pursue a quantitative picture. We have already shown that the speed of amyloid formation is positively correlated with the reaction rates of primary nucleation, elongation, and fragmentation. Such a relationship can be well formulated through the following interesting scaling laws for the apparent fiber growth rate and the half-time for fibrillation (11):

$$\kappa_{1/2}^{fib} \equiv \dot{M}(t_{1/2}) / m_{tot} \propto \left[\left(k_e^+ m_{tot} \right)^{n-1} k_f^+ \right]^{1/n},$$
$$t_{1/2}^{fib} \propto \ln \left[\left(k_f^+ \right)^{2/n} / \left(k_n^+ m_{tot}^{n_c - 1} \right) \right] \left[\left(k_e^+ m_{tot} \right)^{n-1} k_f^+ \right]^{-1/n}, \quad (5)$$

where $t_{1/2}^{fib}$ is determined by $M(t_{1/2}^{fib}) = [M(0) + M(\infty)]/2$.

Whether similar relations are valid for cell damage has not been ascertained. We explore this problem by randomly varying the model parameters that we are most interested in: the protein concentration m_{tot}, the number concentration of oligomers P_{oli}, the reaction rate constants for oligomer binding k_b^+ and unbinding k_b^-, the ion leakage rate k_{leak}, and the ion pumping rate k_{pump}. Those reaction rate constants, which are solely related to amyloid formation, will not be changed.

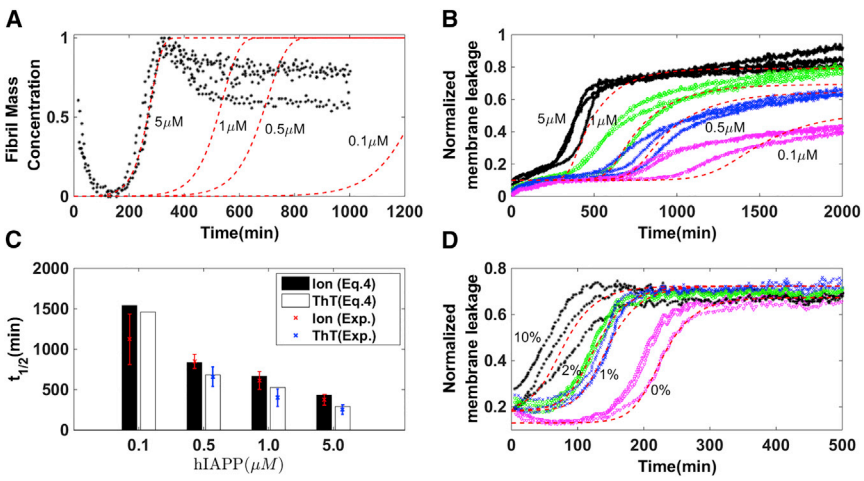

FIGURE 4 Effects of protein and seeds concentration on the kinetics of hIAPP fibril growth and hIAPP-induced membrane leakage: (*A*) fibril mass concentration measured by ThT fluorescence; (*B*) the amount of membrane leakage under different initial protein concentration, which are 5 μM (*black stars*), 1 μM (*green circles*), 0.5 μM (*blue crosses*), and 0.1 μM (*pink triangles*); (*C*) the half-time for fibril formation and membrane leakage; and (*D*) the amount of membrane leakage under different concentrations of seeds, i.e., 0% (*pink triangles*), 1% (*blue crosses*), 2% (*green circles*), and 10% (*black stars*) hIAPP seeds. Experimental data were measured by Engel et al. (42); whereas fitted red lines are given by Eq. 4. Here we set $c_{tot} = 4.3 \times 10^{-5} M$, $k_n^+ = 3 \times 10^{-5} M^{-1} s^{-1}$, $k_e^+ = 10^5 M^{-1} s^{-1}$, $k_f^+ = 7 \times 10^{-5} s^{-1}$, $k_f^- = 10^8 M^{-1} s^{-1}$, $k_b^+ = 4 \times 10^5 M^{-1} s^{-1}$, $k_b^- = 40 M^{-1} s^{-1}$, $k_{pump} = 1.4 \times 10^{-5} M^{-1} s^{-1}$, $k_{leak} = 5 M^{-1} s^{-1}$, $n_c = 2$, $n_o = 40$, $n = 1$, and $k_n^- = k_e^- = 0$. In (*D*), $m_{tot} = 2.5 \times 10^{-5} M$, $k_{pump} = 10^{-4} M^{-1} s^{-1}$, $k_{leak} = 20 M^{-1} s^{-1}$, and $M(0)/P(0) = 400$. How sensitive is the fit to variations of these parameters can be learned through Fig. S1. To see this figure in color, go online.

Through extensive numerical computations (see Fig. S5, for details), the relations for the apparent ion leakage rate and the half-time for ion leakage are found as follows:

$$\kappa_{1/2}^{cell} \equiv \dot{I}_+\left(t_{1/2}^{cell}\right)\Big/ I_+(0) \propto k_{leak}\left[\left(k_b^+ P_{oli}\right)^{-1} + c_0\right]^{-1/2},$$
$$t_{1/2}^{cell} \sim \left(\kappa_{1/2}^{cell}\right)^{-1}, \tag{6}$$

in which $I_+(t_{1/2}^{cell}) = [I_+(0) + I_+(\infty)]/2$ and c_0 is a fitting constant. The first formula in Eq. 6 could also be replaced by $\kappa_{1/2}^{cell} \propto k_{leak}[(k_b^+ m_{tot})^{-1} + c_0]^{-1/2}$, but the agreement becomes a bit poorer. Within the parameter space we explored, no apparent dependence of $\kappa_{1/2}^{cell}$ and $t_{1/2}^{cell}$ on k_b^- and k_{pump} was observed. Besides, both $\kappa_{1/2}^{cell}$ and $t_{1/2}^{cell}$ were found to be independent of the cell concentration c_{tot}, which is consistent with the conclusion of dimensionless analysis. But we note that this result is only valid when linear constitutive relations for ion leakage and pumping are adopted. In the nonlinear region, $\kappa_{1/2}^{cell}$ and $t_{1/2}^{cell}$ should depend on the cell concentration c_{tot} in general.

DISCUSSION

There are many controversies on the possible mechanisms of cell damage caused by amyloid formation. One of representative examples is which form of protein aggregates should be responsible for the cytotoxicity? As we have mentioned in the introduction, for quite a long time mature fibrils were widely taken as the major cause, but this view has been largely changed in the past several years. Now oligomers are considered as the prime pathogenic factor instead. In this study we list four representative mechanisms (see Fig. 5), namely the speed for cell membrane damage (or the speed for changing cells from normal to damaged state in the current model) is directly proportional to 1) the number concentration of oligomers, 2) the mass concentration of oligomers, 3) the number concentration of aggregates, and 4) the mass concentration of aggregates. The difference between Mechanism 1 and Mechanism 2 is based on the interaction way between oligomers and cell membrane. One uses the two ends (like a pin), whereas the other takes the whole surface (like a sticker). Mechanisms 3 and 4 are similar to

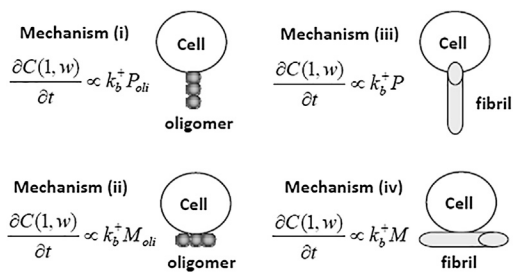

FIGURE 5 An illustration of four possible mechanisms for cell membrane damage.

the first two, except that both oligomers and fibrils are toxic. Based on our own study (mainly through dissecting Figs. 3 and 4, data not shown) and other related experiments (especially those on fiber agitation or sonication), Mechanism 4 is usually excluded. For instance, during agitation M is usually not affected, but cytotoxicity will be changed dramatically. Furthermore, as oligomers generally have a narrow size distribution, it is hard to tell Mechanism 1 from Mechanism 2 by analyzing the results of mathematical models (this difficulty will be left to future experiments and simulations). Finally, in the current model we adopt Mechanism 1 and apply it with great success, but this does not exclude the possibility of the use of Mechanism 3 for other amyloid proteins. Actually both Mechanisms 1 and 3 can be included into a unified model, in which $k_b^+ P_{oli}$ or $k_b^+ P$ is replaced by a comprehensive binding rate function $\sum_{i=n_c}^{\infty} k_b^+(i)[A_i]$. Related studies are left to the future.

It should be noted that in many cases the toxic oligomers are off-pathway aggregates rather than on-pathway precursors or nuclei for fibrils. However, to not go too far away from classical models in this area (8,11,12), as well as to keep the model as simple as possible in the first step, we still model toxic oligomers as on-pathway aggregates and reserve more complicated situations to future studies. Readers should be highly aware of this point.

In this study, a two-state model based on whether the cell is damaged or not is constructed for simplicity. In reality, to account for the different conditions of a cell, a number of states are generally required to achieve a satisfactory description. This problem can be easily solved when a continuous notation $s \in [0, 1]$ is introduced in $C(s, w)$ rather than just 0 and 1. Correspondingly, the last two formulas in Eq. S1 will be replaced by a $2 + 1$D convection equation. Interested readers can find details in the Supporting Material.

The moment-closure method based on the maximum entropy principle plays a key role in model reduction. Especially the entropy function that we adopted in Eq. S5 directly determines the accuracy of the reduced model. To make the static values of $P(t)$, $[C_+(t) - C_-(t)]/(2c_{tot})$, and $1 - I_+(t)/c_{tot}$ closer to their exact solutions than what have been shown in Fig. 2, *A–D*, a more accurate entropy function should be considered. For example, an alternative entropy function $S = k_B \sum_{i=1}^{\infty}([A_i]\ln[A_i] - [A_i]) - k_B(\mathrm{n} - 1)\sum_{i=1}^{\infty} \ln i \times [A_i]$ has been considered in our previous study (14). Another issue is related to the self-closure of last three formulas in Eq. 4, which is based on the particular choice of linear constitutive relations as we have shown in the Supporting Material. Once the nonlinearity of ion leakage and ion pumping is considered, high-order moments will be involved automatically. Under that condition, additional moment-closure methods must be introduced similarly to what we have done for the mass-action equations. Related studies are still being conducted.

In conclusion, this study examined the problem of cell damage caused by amyloid formation. Based on four simple

assumptions, one of which is that cell damage is raised by oligomers rather than mature fibrils, we constructed a microscopic mathematical model that consists of infinite ODEs in the form of mass-action equations together with two reaction-convection PDEs. This model then was simplified into a macroscopic system of five ODEs by using the maximum entropy principle. With the simplified model, the effects of primary nucleation, elongation, fragmentation, and protein and seeds concentration on amyloid formation and cell damage were extensively explored and compared with the experiments. We hope that our results can provide quantitative insights into the roles of oligomers played during cell damage, which is a prerequisite for understanding the occurrence, progression, and deterioration of amyloid diseases.

SUPPORTING MATERIAL

Supporting Materials and Methods, five figures, and fifteen equations are available at http://www.biophysj.org/biophysj/supplemental/S0006-3495(15)00817-6.

AUTHOR CONTRIBUTIONS

L.H. designed the studies. L.H. and W.Y. developed the model. L.H. and Y.H. performed the numerical simulations. Y.H., L.H., and W.Y. wrote the article together. All authors gave final approval for publication.

ACKNOWLEDGMENTS

We are indebted to three anonymous reviewers for providing detailed and insightful comments. Without their supportive work, this article would not have been possible.

This work was supported by the National Natural Science Foundation of China (Grants 11204150 and 11471185) and by the Tsinghua University Initiative Scientific Research Program (Grants 20121087902 and 20131089184). L.H. also acknowledges the Erasmus Mundus Master Programme in System Biology from Aalto University, Finland.

REFERENCES

1. Prusiner, S. B. 1982. Novel proteinaceous infectious particles cause scrapie. *Science.* 216:136–144.
2. Chiti, F., and C. M. Dobson. 2006. Protein misfolding, functional amyloid, and human disease. *Annu. Rev. Biochem.* 75:333–366.
3. Oosawa, F., S. Asakura, and T. Ooi. 1959. G-F transformation of action as a fibrous condensation. *J. Polym. Sci.* 37:323–336.
4. Morris, A. M., M. A. Watzky, and R. G. Finke. 2009. Protein aggregation kinetics, mechanism, and curve-fitting: a review of the literature. *Biochim. Biophys. Acta.* 1794:375–397.
5. Hofrichter, J., P. D. Ross, and W. A. Eaton. 1974. Kinetics and mechanism of deoxyhemoglobin S gelation: a new approach to understanding sickle cell disease. *Proc. Natl. Acad. Sci. USA.* 71:4864–4868.
6. Ferrone, F. A., J. Hofrichter, …, W. A. Eaton. 1980. Kinetic studies on photolysis-induced gelation of sickle cell hemoglobin suggest a new mechanism. *Biophys. J.* 32:361–380.
7. Ruschak, A. M., and A. D. Miranker. 2007. Fiber-dependent amyloid formation as catalysis of an existing reaction pathway. *Proc. Natl. Acad. Sci. USA.* 104:12341–12346.
8. Oosawa, F., and S. Asakura. 1975. Thermodynamics of the Polymerization of Protein. Academic Press, New York.
9. Collins, S. R., A. Douglass, …, J. S. Weissman. 2004. Mechanism of prion propagation: amyloid growth occurs by monomer addition. *PLoS Biol.* 2:e321.
10. Xue, W.-F., A. L. Hellewell, …, S. E. Radford. 2009. Fibril fragmentation enhances amyloid cytotoxicity. *J. Biol. Chem.* 284:34272–34282.
11. Hong, L., and W. A. Yong. 2013. Simple moment-closure model for the self-assembly of breakable amyloid filaments. *Biophys. J.* 104: 533–540.
12. Knowles, T. P. J., C. A. Waudby, …, C. M. Dobson. 2009. An analytical solution to the kinetics of breakable filament assembly. *Science.* 326:1533–1537.
13. Cohen, S. I. A., M. Vendruscolo, …, T. P. J. Knowles. 2012. From macroscopic measurements to microscopic mechanisms of protein aggregation. *J. Mol. Biol.* 421:160–171.
14. Tan, P., and L. Hong. 2013. Modeling fibril fragmentation in real-time. *J. Chem. Phys.* 139:084904.
15. Dobson, C. M. 2003. Protein folding and misfolding. *Nature.* 426: 884–890.
16. Haass, C., and D. J. Selkoe. 2007. Soluble protein oligomers in neurodegeneration: lessons from the Alzheimer's amyloid β-peptide. *Nat. Rev. Mol. Cell Biol.* 8:101–112.
17. De Simone, A., L. Esposito, …, L. Vitagliano. 2008. Insights into stability and toxicity of amyloid-like oligomers by replica exchange molecular dynamics analyses. *Biophys. J.* 95:1965–1973.
18. Bolognesi, B., J. R. Kumita, …, J. J. Yerbury. 2010. ANS binding reveals common features of cytotoxic amyloid species. *ACS Chem. Biol.* 5:735–740.
19. Olzscha, H., S. M. Schermann, …, R. M. Vabulas. 2011. Amyloid-like aggregates sequester numerous metastable proteins with essential cellular functions. *Cell.* 144:67–78.
20. Williams, T. L., and L. C. Serpell. 2011. Membrane and surface interactions of Alzheimer's Aβ peptide–insights into the mechanism of cytotoxicity. *FEBS J.* 278:3905–3917.
21. Wong, P. T., J. A. Schauerte, …, A. Gafni. 2009. Amyloid-beta membrane binding and permeabilization are distinct processes influenced separately by membrane charge and fluidity. *J. Mol. Biol.* 386:81–96.
22. Capone, R., F. G. Quiroz, …, M. Mayer. 2009. Amyloid-beta-induced ion flux in artificial lipid bilayers and neuronal cells: resolving a controversy. *Neurotox. Res.* 16:1–13.
23. Kawahara, M. 2010. Neurotoxicity of β-amyloid protein: oligomerization, channel formation, and calcium dyshomeostasis. *Curr. Pharm. Des.* 16:2779–2789.
24. Demuro, A., M. Smith, and I. Parker. 2011. Single-channel $Ca(^{2+})$ imaging implicates Aβ1-42 amyloid pores in Alzheimer's disease pathology. *J. Cell Biol.* 195:515–524.
25. Schauerte, J. A., P. T. Wong, …, A. Gafni. 2010. Simultaneous single-molecule fluorescence and conductivity studies reveal distinct classes of Abeta species on lipid bilayers. *Biochemistry.* 49:3031–3039.
26. Ono, K., M. M. Condron, and D. B. Teplow. 2009. Structure-neurotoxicity relationships of amyloid beta-protein oligomers. *Proc. Natl. Acad. Sci. USA.* 106:14745–14750.
27. Fändrich, M. 2012. Oligomeric intermediates in amyloid formation: structure determination and mechanisms of toxicity. *J. Mol. Biol.* 421:427–440.
28. Cohen, S. I. A., S. Linse, …, T. P. J. Knowles. 2013. Proliferation of amyloid-β42 aggregates occurs through a secondary nucleation mechanism. *Proc. Natl. Acad. Sci. USA.* 110:9758–9763.
29. Pallitto, M. M., and R. M. Murphy. 2001. A mathematical model of the kinetics of *beta*-amyloid fibril growth from the denatured state. *Biophys. J.* 81:1805–1822.
30. Manno, M., E. F. Craparo, …, P. L. San Biagio. 2007. Kinetics of different processes in human insulin amyloid formation. *J. Mol. Biol.* 366:258–274.

31. Schreck, J. S., and J. M. Yuan. 2013. A kinetic study of amyloid formation: fibril growth and length distributions. *J. Phys. Chem. B.* 117:6574–6583.

32. Serio, T. R., A. G. Cashikar, …, S. L. Lindquist. 2000. Nucleated conformational conversion and the replication of conformational information by a prion determinant. *Science.* 289:1317–1321.

33. van der Linden, E., and P. Venema. 2007. Self-assembly and aggregation of proteins. *Curr. Opin. Colloid Interface Sci.* 12:158–165.

34. Powers, E. T., and D. L. Powers. 2008. Mechanisms of protein fibril formation: nucleated polymerization with competing off-pathway aggregation. *Biophys. J.* 94:379–391.

35. Doran, T. M., E. A. Anderson, …, B. L. Nilsson. 2012. Turn nucleation perturbs amyloid β self-assembly and cytotoxicity. *J. Mol. Biol.* 421:315–328.

36. Lorenzen, N., S. B. Nielsen, …, D. E. Otzen. 2014. The role of stable α-synuclein oligomers in the molecular events underlying amyloid formation. *J. Am. Chem. Soc.* 136:3859–3868.

37. Hill, T. L. 1983. Length dependence of rate constants for end-to-end association and dissociation of equilibrium linear aggregates. *Biophys. J.* 44:285–288.

38. Stefani, M. 2013. The oligomer species: mechanistics and biochemistry. *In* Amyloid Fibrils and Prefibrillar Aggregates: Molecular and Biological Properties. D. K. Otzen, editor. Wiley, Weinheim, Germany.

39. Wang, Y. Q., A. K. Buell, …, S. Perrett. 2011. Relationship between prion propensity and the rates of individual molecular steps of fibril assembly. *J. Biol. Chem.* 286:12101–12107.

40. Xue, W. F., A. L. Hellewell, …, S. E. Radford. 2010. Fibril fragmentation in amyloid assembly and cytotoxicity: when size matters. *Prion.* 4:20–25.

41. Bucciantini, M., E. Giannoni, …, M. Stefani. 2002. Inherent toxicity of aggregates implies a common mechanism for protein misfolding diseases. *Nature.* 416:507–511.

42. Engel, M. F. M., L. Khemtémourian, …, J. W. M. Höppener. 2008. Membrane damage by human islet amyloid polypeptide through fibril growth at the membrane. *Proc. Natl. Acad. Sci. USA.* 105:6033–6038.